BPR MCS Bulletin of Pioneering Researches of Medical and Clinical Science

Bulletin of Pioneering Researches of Medical and Clinical Science

Available online: https://bprmcs.com
2024 | Volume 4 | Issue 1 | Page: 168-185

Therapeutic Effects of Goose Deoxycholic Acid on FLHS-Induced Liver Injury via Macrophage Polarization and Inflammatory Response Suppression

Michael Turner[1], Sophia Nguyen[2]*, David Clark[1], Emma Wilson[3]

[1]Department of Clinical Research and Medical Innovation, Faculty of Medicine, University of Glasgow, Glasgow, United Kingdom.
[2]Department of Translational Medical Sciences, National University of Singapore, Singapore.
[3]Department of Clinical Investigation and Biomedical Systems, University of Sydney, Sydney, Australia.

Abstract

Fatty liver hemorrhagic syndrome (FLHS) affecting laying hens represents a metabolic-nutritional condition whose principal manifestations include liver enlargement, lipid accumulation within hepatocytes, and intrahepatic bleeding. This disorder tends to emerge during the phase of maximal egg production, causing substantial financial setbacks for the poultry sector; however, the exact mechanisms driving FLHS remain poorly understood. Investigations conducted by our team, along with earlier reports, have revealed that concentrations of bile acids drop considerably as fatty liver progresses, and that purposeful stimulation of signaling cascades involving bile acids can assist in both averting and managing fatty liver. For the current work, we produced an FLHS model in laying hens by administering a diet rich in energy but low in protein, while supplying goose deoxycholic acid (CDCA) as a therapeutic measure. Hematoxylin-eosin staining, fluorescence-based quantitative PCR, and ELISA techniques were applied to gauge CDCA's influence on hepatic pathological alterations and inflammatory processes. Outcomes revealed a noticeable reduction in hepatic bleeding among FLHS-affected hens receiving CDCA. Similarly, fatty vacuoles and circulating transaminase enzymes declined markedly. Beyond this, indicators of M1-polarized macrophages and their secretory products were sharply downregulated, and mediators promoting inflammation tied to the JAK-STAT cascade, the LPS-TLR4-Myd88–NF-kB axis, and NLRP3 inflammasome assembly were also substantially diminished. Conversely, markers of M2-polarized macrophages and their associated products rose notably, paralleled by heightened expression of anti-inflammatory components associated with the JAK-STAT pathway. Collectively, these findings indicate that CDCA mitigates hepatic damage in FLHS laying hens by restraining M1-type macrophage polarization and the accompanying pro-inflammatory cascade, while simultaneously encouraging M2-type polarization and an inflammation-resolving response.

Keywords: Goose deoxycholic acid, M1-type polarization, M2-type polarization, Liver damage, FLHS laying hens

Corresponding author: Sophia Nguyen
E-mail: sophia.nguyen@gmail.com

How to Cite This Article: Turner M, Nguyen S, Clark D, Wilson E. Therapeutic Effects of Goose Deoxycholic Acid on FLHS-Induced Liver Injury via Macrophage Polarization and Inflammatory Response Suppression. Bull Pioneer Res Med Clin Sci. 2024;4(1):168-85. https://doi.org/10.51847/AU7GFACg1r

Introduction

Fatty liver hemorrhagic syndrome (FLHS) in laying hens, originally described and designated by Couch in 1956, constitutes a nutritionally rooted metabolic disturbance defined by hepatic bleeding and steatosis [1]. Predisposing factors span genetics, dietary factors, environmental factors, and additional aspects such as husbandry

practices. The malady typically strikes caged layers in prime physical condition during the egg-laying zenith, and its onset can precipitate a decline in egg productivity. Under the conditions of contemporary intensive production, FLHS pathogenesis correlates mainly with excessive caloric intake from feed. Even though the detailed pathogenic cascade is not yet resolved, the pathological features parallel those seen in non-alcoholic fatty liver disease. The "second strike" concept advanced by Day and James [2] in 1998 stands as the presently recognized plausible framework for non-alcoholic fatty liver disease (NAFLD). According to this model, the initial strike entails a surplus deposition of triglycerides and unesterified fatty acids in hepatic tissue due to excessive lipid intake, culminating in steatosis. The compromised resilience of fatty hepatocytes subsequently elicits oxidative stress responses. The subsequent strike encompasses the compounded effects of oxidative imbalance, mitochondrial dysfunction, and hepatic inflammatory responses, all of which amplify the repercussions of the initial strike and thereby intensify hepatic injury.

The intrahepatic inflammatory response is predominantly orchestrated by resident hepatic macrophages. When stimulated, these macrophages can differentiate into either an M1 or an M2 phenotype. Recent investigations have documented that engagement of the TLR4 receptor situated on the outer membrane of hepatic macrophages by LPS steers their skewing toward the M1 phenotype, after which they release a suite of pro-inflammatory mediators, prominently including interleukin (IL)-1, tumor necrosis factor–alpha (TNF-alpha), and reactive oxygen intermediates, which are capable of provoking inflammation-mediated hepatic damage [3]. The canonical understanding posits that LPS challenge initiates hepatic inflammatory pathology, and that as hepatic inflammation unfolds, IL-4 binding to macrophage surface receptors activates JAK, facilitates STAT phosphorylation, and redirects macrophage polarization toward the M2 phenotype, dampening the pro-inflammatory cascade and easing hepatic injury [4]. M2-skewed macrophages release bioactive substances such as IL-4 and IL-10 that moderate inflammation whilst also triggering programmed cell death of M1-polarized macrophages, thereby lessening hepatic inflammatory damage.

A growing body of contemporary literature has substantiated that the physiological activities of bile acids manufactured by the liver hold considerable sway over lipid handling, sugar metabolism, and inflammatory regulation, among other roles, by engaging the farnesol X receptor and G protein–coupled receptor [5]. Even though the work by Oleszycka Ewa *et al*. underscored the capacity of bile acids at physiological levels to promote the generation of pro-inflammatory mediators and mobilize innate immune cells during the course of inflammatory conditions [6], a substantial body of recent evidence has shown that exogenously dosed bile acids can successfully curb inflammation under pathological circumstances. Prior investigations by our research group have revealed that bile acid composition shifts dramatically in the context of FLHS, with CDCA titers declining particularly sharply. Accordingly, preventive supplementation with CDCA can impede FLHS development. It has been noted that the bile acid membrane receptor G protein–coupled receptor 5 (TGR5) appears predominantly on the outer face of macrophage membranes, and CDCA happens to be a key ligand for TGR5. Separate studies have indicated that bile acid coupling to TGR5 produces meaningful anti-inflammatory effects. At the same time, other reports have documented that CDCA exerts anti-inflammatory effects by activating the TGR5 signaling pathway [7, 8]. We therefore hypothesized that CDCA administration could alleviate hepatic damage by reshaping macrophage-driven inflammatory processes in the livers of FLHS-stricken laying hens.

In the present study, we established an FLHS model in laying hens by providing high-energy/low-protein rations and supplementing them with CDCA to assess its impact on liver injury, pro-inflammatory cascades driven by M1 macrophage polarization, and inflammation-counteracting responses driven by M2 macrophage polarization. The overarching purpose of this investigation was to tease apart the modulatory influence of CDCA on inflammation-associated hepatic injury in FLHS laying hens and its plausible mechanistic underpinnings, thereby furnishing a conceptual foundation for deploying CDCA in FLHS prophylaxis and therapy in laying flocks.

Materials and Methods

Experimental design

The study utilized 216 Hyland Brown laying hens at 26 weeks of age (representing the peak laying stage) with comparable body weights. The foundational ration was composed according to NRC (1998) guidelines. The high-energy, protein-restricted feed incorporated the following ingredients: corn: 35–45%, millet polished meal: 5–15%, pepper seeds: 3–8%, soybean meal: 4–7%, stone pellets: 8–10%, citric acid residue: 1–3%, corn sugar residue: 1–5%, peanut cake: 1–6%, corn germ cake: 3–6%, sesame seed cake: 1–7%, soybean oil: 0.5–1%, beet molasses: 1–2%. Calcium Hydrogen Phosphate: 0.5–0.8%, 60% Choline Chloride: 0.1–0.2%, Sodium Chloride: 0.25–0.35%, Amino Acids: 0.25–0.85%, Mineral Premix: 0.2%, Vitamin Premix: 0.2%. CDCA was obtained from Hebei Huaheng Biotechnology Co, LTD, Hebei, China. The birds were housed in three-dimensional cage systems used in commercial egg-laying operations and were maintained

under husbandry conditions identical to those on production farms. The indoor environment of the henhouse was maintained at 21–25 °C, with relative humidity between 45% and 65%, and a full disinfection cycle was performed once every 7 days. The flock also underwent all standard immunization protocols.

After an initial adaptation period of approximately 1 week, birds that demonstrated minimal variation among individuals, satisfactory physical fitness, and an absence of clinical abnormalities or disease indicators were chosen and then assigned at random into six experimental groups, each consisting of three replicates housing twelve hens apiece; the specific grouping design and corresponding interventions are detailed in **Table 1**. At the conclusion of the feeding trial, blood specimens were taken and spun to separate serum, following which the hens were humanely sacrificed and their livers harvested for subsequent analytical procedures. All methodologies employed in the animal experimentation were scrutinized and given official clearance before commencement by the Animal Care and Use Committee of Shenyang Agricultural University (approval no. 2019030101).

Table 1. Animal groups and treatments.

Experimental group	Sample size (n)	Dietary intervention
Control group (C)	n = 36	Corn–soybean meal–based diet
FLHS model group (M)	n = 36	A diet high in energy and low in protein
Low-dose CDCA group (CDCA L)	n = 36	High-energy, low-protein diet supplemented with 0.01% CDCA
Medium-dose CDCA group (CDCA M)	n = 36	High-energy, low-protein diet supplemented with 0.02% CDCA
High-dose CDCA group (CDCA H)	n = 36	High-energy, low-protein diet supplemented with 0.03% CDCA
Control + CDCA group (CC)	n = 36	Corn–soybean meal–based diet with 0.02% CDCA supplementation

Histopathological analysis

Portions of hepatic tissue excised from the laying hens were submerged in 4% paraformaldehyde solution for fixation, then withdrawn from the specimen containers and taken through the following steps for histopathological preparation: the tissue pieces were rinsed, passed through graded dehydration stages, cleared of dehydrant, infiltrated with molten paraffin, and embedded into blocks, and finally sliced into thin sections and mounted onto glass slides. Every step was performed in strict adherence to the manufacturer's directions enclosed with the HE staining kit. Once the staining procedure was completed, the tissue sections were sealed beneath coverslips using neutral balsam, permitted to dry thoroughly, and visualized using a light microscope.

Determination of serum biochemical indices

Serum specimens were processed to measure the enzymatic activities of ALT and AST using the colorimetric assay method as described in the instructional manual provided with the detection kit (Nanjing Jiancheng Bioengineering Institute, Nanjing, China).

Detection of inflammatory factors in liver tissue

The intrahepatic concentrations of IL-1β, IL-6, TNF-α, IFN-γ, IL-4, and IL-10 in the experimental laying hens from every group were evaluated through a multiplex immunoassay platform. A commercially sourced ELISA kit (Nanjing Jiancheng Bioengineering Institute, China) was used to measure hepatic levels of IL-8, IL-18, and inducible nitric oxide synthase (iNOS) across the experimental hen groups.

Real-time polymerase chain reaction (PCR) analysis

Total cellular RNA was isolated from hepatic tissue samples using TRIzol extraction reagent, and the purity of the harvested RNA was assessed using a microplate spectrophotometer. The absorbance ratio at 260 nm to 280 nm was recorded after the instrument was zeroed against double-distilled water. Values within the 1.8–2.0 interval indicated that the RNA purity was adequate for the downstream experiments. The isolated RNA was then converted to complementary DNA using a reverse transcription kit, exactly as directed by the supplier's protocol.

Transcript abundance of the targeted gene products was determined using real-time quantitative PCR methodology. Complete nucleotide sequences for the genes of interest were obtained from the GenBank database hosted on NCBI, and Primer Premier 5 was used to generate primer sequences, which are listed in **Table 2**. Once the specificity of each primer pair was validated as acceptable, SYBR Green II fluorescent dye was used for real-time quantitative PCR, with β-actin as the housekeeping reference gene to standardize target gene expression measurements. The resulting mRNA expression data were calculated using the $2^{-\Delta\Delta CT}$ quantification approach.

Table 2. Primer sequences used for fluorescence quantitative real-time PCR.

Gene	Primer sequences		ID
iNOS	F: ATCTACAGGTATTGATGCTCGT	R: TTCTGGATCTTGGCCGTTTG	35671
JAK2	F: CTGGCTTCTACGTTCTTCGT	R: GGAGGTTTGATTTATCTTTTGG	374199

STAT1	F: TACTTATGACCCTGACCCTATC	R: TTTCCTGAATCCTTTGACTG	424044
IRF5	F: ATCCAAGTGTTCAGCCTCCA	R: CTCCACCAGAGCATCCTTCA	430409
TLR4	F: GGAGGTTGTAGATTTGATGAG	R: AGATGGGACATAACATGATTT	417241
MyD88	F: GAGTTGGAGCAAACGGAGTT	R: TTGGTGCAAGGATTGGTGTA	420420
NF-κB	F: AGGTGGTCCCTAAGTTCCGTG	R: TTTGCCTCTTGGTGCGTTTC	396093
AP-1	F: AACTTCGTGCCCACCGTGAC	R: CCGCTGCCATCTTGTTCCTC	102587711
IRF1	F: AGCATTGAGGATATCGTGAAG	R: TGGTTGTGGTCTGTGCTGTGT	396384
NLRP3	F:AAAGGACGTGAATATGTTGTTA	R: CAAGGCTATTCCTGTGAAACT	423021
Caspase-1	F: GCTGCCGTGGAGACAACATA	R: CGTTGGACCTTTCGGAACAT	395764
Caspase-11	F: AGTCAGAGCACAGGACGAAG	R: GATGGGAAGAGGAAGAGAG	395476
CD163	F: TGGTTCCGCTCATTTTGGTC	R: GGGCAGTTTCAGTTCCTTTAC	426826
CD206	F: GCATCAAGCGTATTTAGCAA	R: GAAAGTCCAATCCAAAAGTAT	9332
ARG	F: TGATCTTGGAGTCATCTGGG	R: GTCCGTCAACATCAAAACTTAG	46717
IL-4R	F: CAGCATCACCAAGATTAGAA	R: TCCAGAAAACAGGGCAAGAG	3566
STAT6	F: CTGGGAGAAGATGTGCGATAC	R: TTGCTGATGAAGCCAATGAT	100859196
SOCS1	F: CGATGTCTACTTGACCCTCC	R: CCCCGTCTGAAAGTTTATCC	416630
PPARy	F: GCAGGAACAGAACAAAGAAG	R: TGCCAGGTCACTGTCATCTA	100356422
KLF4	F: CCTTCAACCTGGCGGACATC	R: CTGGCCTCCTGCTTGATTTT	770254
β-Actin	F: GGAGGGAAATCGTGCGTGACA	R: CGATAGTGACCTGACCGTCA	396526

Statistical analysis

The collected data were processed using SPSS 23.0. Between-group differences were assessed for statistical significance through one-way analysis of variance. The LSD method was applied for conducting multiple comparisons. Results are reported as the mean accompanied by the standard error of the mean (SEM). A threshold of $P < 0.05$ was adopted to denote statistical significance.

Results and Discussion

CDCA mitigates the consequences of hepatic injury

Figure 1 presents a histological depiction of hepatic tissue obtained from an experimental hen. The livers from laying hens belonging to Group C displayed a sleek and lustrous exterior, a resilient consistency, and a typical dark-red hue devoid of any bleeding indications. In contrast, the livers from Group M hens exhibited an earthy-yellow discoloration, a yielding texture, disintegrated readily when compressed between the fingers, and showed extensive regions of surface hemorrhage or coagulated blood. Hepatic surface bleeding in the laying hens was substantially reduced through CDCA administration, mirroring the observations recorded for Group C. One diagnostic hallmark of FLHS is the presence of numerous hemorrhagic foci or blood clots across the hepatic surface. The successful establishment of the FLHS model could be verified by visual assessment of the liver during postmortem examination. Incorporating CDCA into the feed successfully diminished the incidence of FLHS.

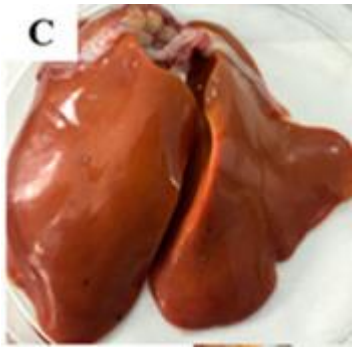

a)

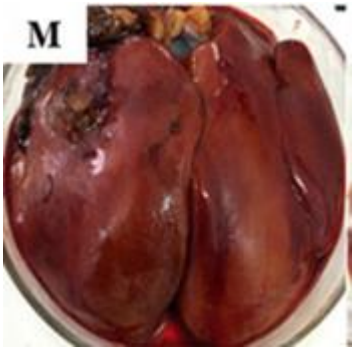

b)

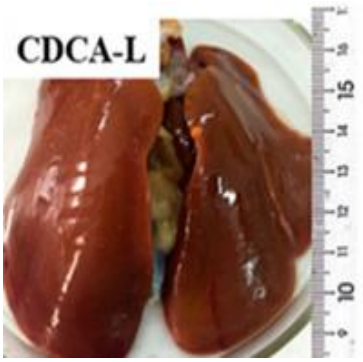

c)

Figure 1. Gross appearance of laying hen livers.

Circulating concentrations of alanine aminotransferase (ALT) and aspartate aminotransferase (AST) in the experimental laying hens were markedly elevated in the FLHS model group relative to the normal group **(Figure 2)**($P < 0.05$), and supplementation with CDCA drove these levels down even further ($P < 0.01$).

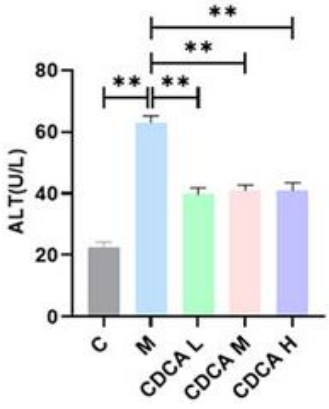

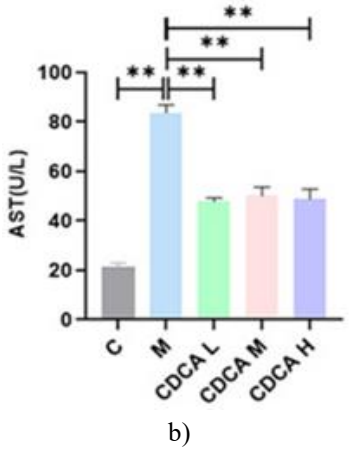

Figure 2. Hepatic function parameters in laying hens: (a) Influence of CDCA supplementation on serum ALT concentrations in FLHS laying hens, and (b) Influence of CDCA supplementation on serum AST concentrations in FLHS laying hens. Values are presented as mean ± SEM. $P < 0.01$.

The findings from HE staining of hepatic tissue sections obtained from experimental laying hens are displayed in **Figure 3**. Within the normal control group, hepatocyte cord arrangements were distinctly observable, and no lipid droplets were detected. Compared with the control group, a portion of the hepatocyte cord architecture in liver sections from the FLHS group had disappeared, and characteristic features of hepatic steatosis were apparent. Moreover, fat vacuoles appeared prominent in both dimensions and abundance, and based on these observations, the successful establishment of the FLHS model was concluded. Lipid vacuoles within hepatocytes decreased in size and became less numerous following CDCA administration, indicating significant amelioration relative to Group M.

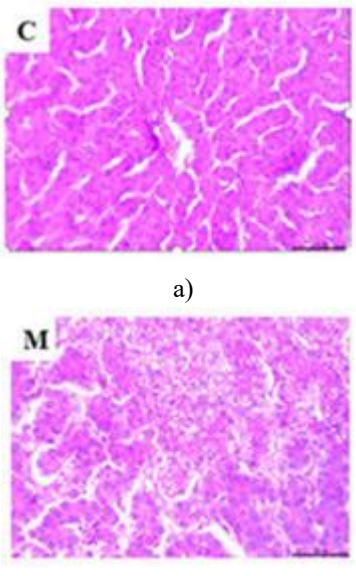

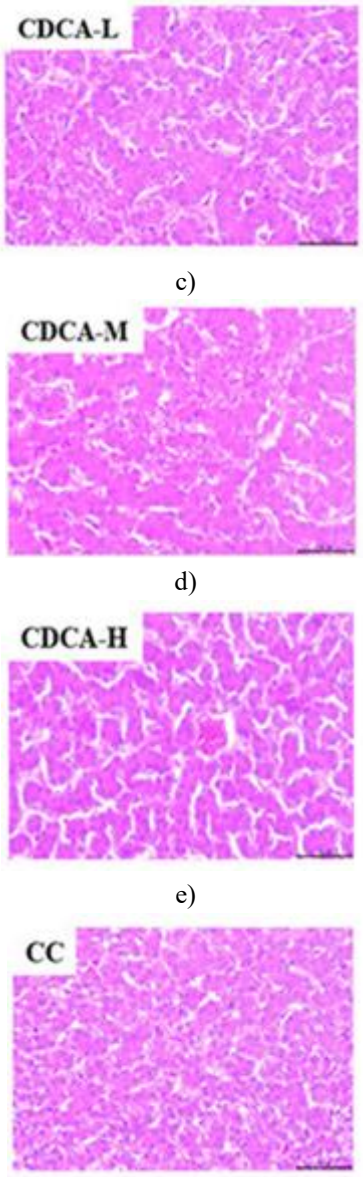

Figure 3. Microscopic evaluation of hepatic tissue sections from laying hens (HE 400×).

CDCA attenuates the pro-inflammatory cascade arising from M1-type macrophage polarization

The findings from the assessment of hepatic M1 macrophage markers in laying hens are displayed in **Figure 4**. Transcript levels of CD68 and iNOS were substantially elevated in the FLHS model cohort compared with the normal control cohort ($P < 0.01$). Upon treatment with CDCA, transcript abundance of both CD68 and iNOS declined significantly compared with the control cohort ($P < 0.01$).

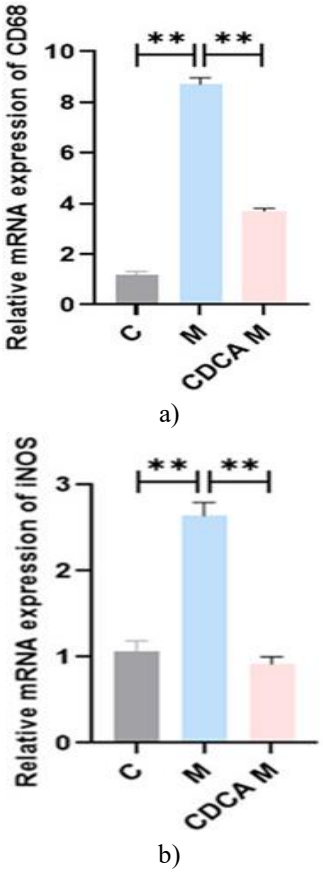

Figure 4. Profiling of macrophage indicators within the livers of laying hens: (a) Impact of CDCA administration on CD68 transcript levels in FLHS-affected laying hens, and (b) Impact of CDCA administration on iNOS transcript levels in FLHS-affected laying hens. All values are given as mean ± SEM. $P < 0.01$.

The relative abundance of molecular mediators tied to M1-polarized macrophages is depicted in **Figure 5**. Quantities of IL-1β, IL-6, IL-8, IL-18, iNOS, and TNF-α rose to a highly statistically significant degree in the FLHS model set when set against the healthy control set ($P < 0.01$). Following CDCA intervention, each of these measured parameters fell considerably below the levels observed in the control set ($P < 0.01$).

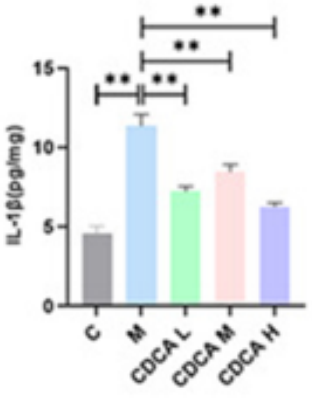

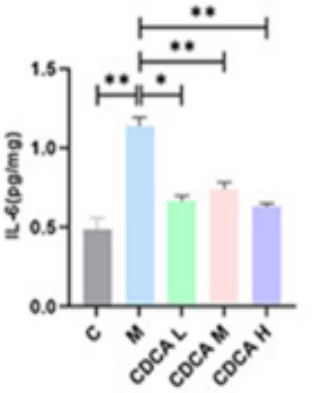

b)

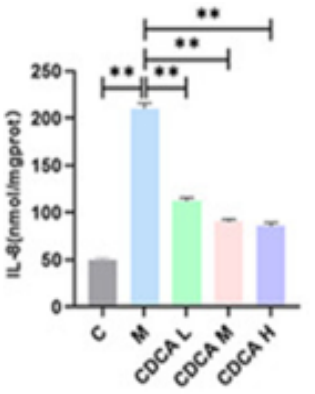

c)

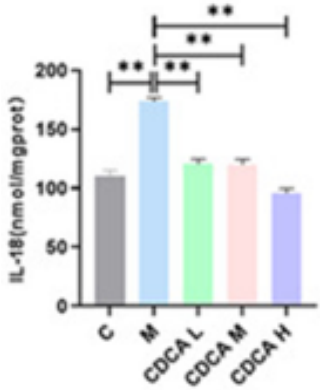

d)

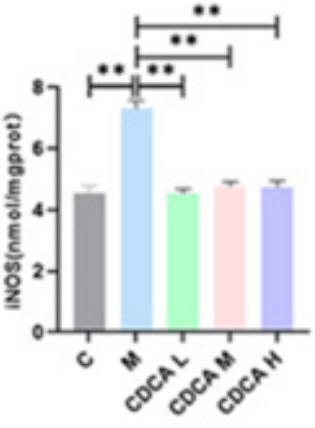

e)

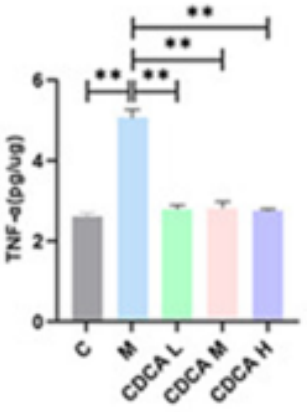

f)

Figure 5. Measurement of inflammation-promoting factors in the hepatic tissue of laying hens: (a) CDCA's effect on intrahepatic IL-1β concentrations in FLHS hens, (b) CDCA's effect on intrahepatic IL-6 concentrations in FLHS hens, (c) CDCA's effect on intrahepatic IL-8 concentrations in FLHS hens, (d) CDCA's effect on intrahepatic IL-18 concentrations in FLHS hens, (e) CDCA's effect on intrahepatic iNOS concentrations in FLHS hens, and (f) CDCA's effect on intrahepatic TNF-α concentrations in FLHS hens. All data plotted as mean ± SEM. $P < 0.05$ and $P < 0.01$.

The findings from the scrutiny of downstream elements of M1-polarized macrophages are illustrated in **Figure 6**. The mRNA copy numbers corresponding to JAK2, STAT1, and IRF5—which function as regulatory nodes in the transduction pathway triggered by IFN-γ—were found at significantly greater abundance within the FLHS model set when measured against the untreated normal set ($P < 0.01$). Intervention with CDCA led to a pronounced drop in IFN-γ expression ($P < 0.01$) and, likewise, reduced mRNA levels of JAK2, STAT1, and IRF5 ($P < 0.01$).

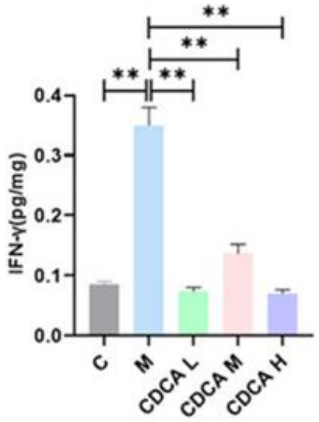

a)

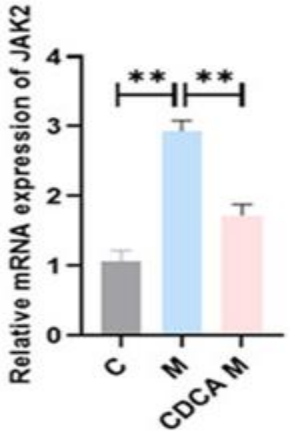

b)

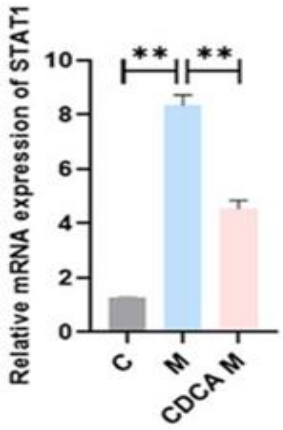

c)

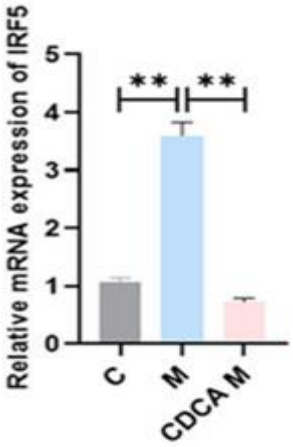

d)

Figure 6. Profiling of molecular participants tied to the signaling cascade downstream of M1-polarized macrophages: (a) Alterations in intrahepatic IFN-γ content following CDCA supplementation in FLHS hens, (b) Alterations in JAK2 transcript expression within the liver following CDCA supplementation in FLHS hens, (c) Alterations in STAT1 transcript expression within the liver following CDCA supplementation in FLHS hens, and (d) Alterations in IRF5 transcript expression within the liver following CDCA supplementation in FLHS hens. Measurements are reported as mean ± SEM. $P < 0.01$.

The assessment of the LPS-TLR4-MyD88–NF-κB pro-inflammatory signaling route yielded the data depicted in **Figure 7**. In contrast to the normal group, LPS titers were substantially elevated in the FLHS model group ($P < 0.01$), accompanied by notable upregulation of the mRNAs encoding TLR4, MyD88, NF-κB, AP-1, and IRF1 ($P < 0.01$). Treatment with CDCA resulted in a pronounced reduction in LPS titers ($P < 0.01$) and a significant decline in transcript levels of TLR4, MyD88, NF-κB, AP-1, and IRF1 ($P < 0.01$).

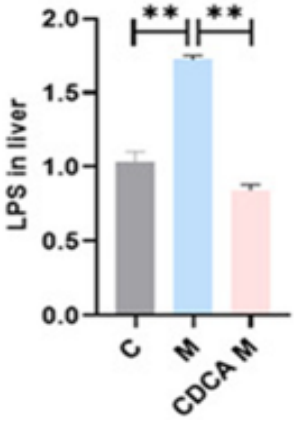

a)

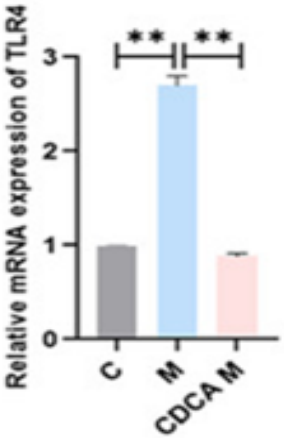

b)

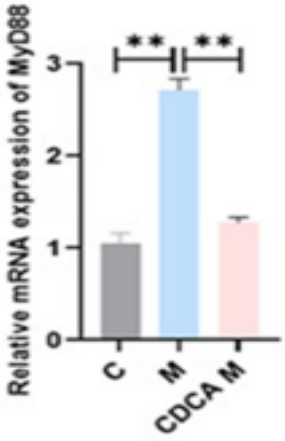

c)

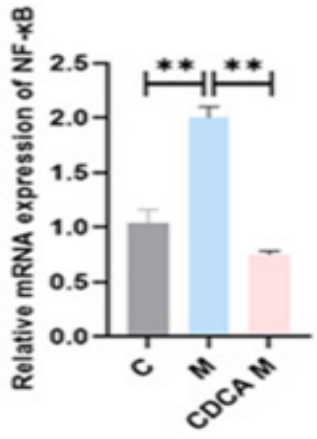

d)

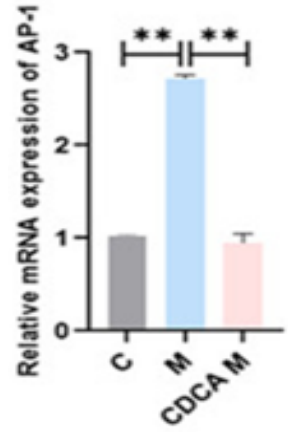

e)

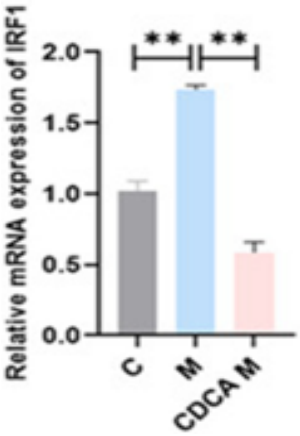

f)

Figure 7. Dissection of the LPS-TLR4-MyD88-NF-κB inflammatory signaling axis: (a) Alteration in LPS titers within FLHS hens following CDCA administration, (b) Alteration in TLR4 gene transcript expression within FLHS hens following CDCA administration, (c) Alteration in MyD88 gene transcript expression within FLHS hens following CDCA administration, (d) Alteration in NF-κB gene transcript expression within FLHS hens following CDCA administration, (e) Alteration in AP-1 gene transcript expression within FLHS hens following CDCA administration, and (f) Alteration in IRF1 gene transcript expression within FLHS hens following CDCA administration. Data plotted as mean ± SEM. $P < 0.01$.

The analytical outcomes for factors linked to the NLRP3 inflammasome complex are depicted in **Figure 8**. The abundance of transcripts coding for NLRP3, Caspase1, and Caspase11 rose sharply in the FLHS model set when contrasted against the normal control set ($P < 0.01$). Upon CDCA supplementation, the expression of NLRP3, Caspase1, and Caspase11 mRNA transcripts decreased significantly compared with the control set ($P < 0.01$).

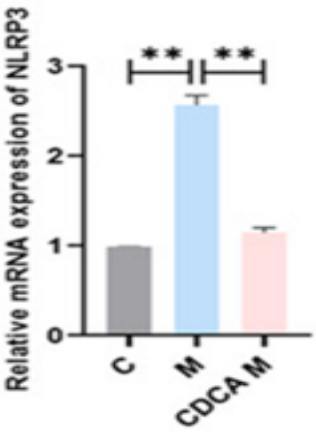

a)

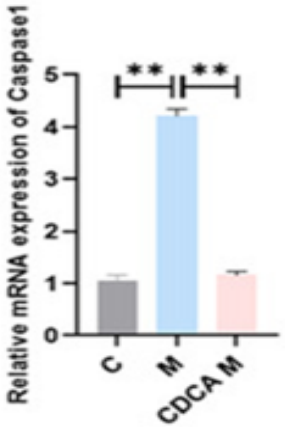

b)

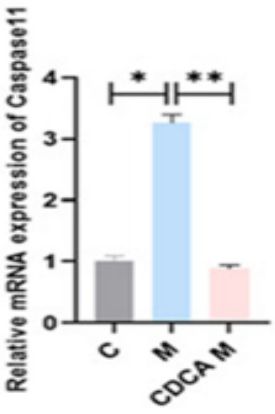

c)

Figure 8. Profiling of components associated with the NLRP3 inflammasome machinery: (a) Changes in hepatic NLRP3 transcript levels after CDCA

supplementation in FLHS hens, (b) Changes in hepatic Caspase1 transcript levels after CDCA supplementation in FLHS hens, and (c) Changes in hepatic Caspase11 transcript levels after CDCA supplementation in FLHS hens. Results are displayed as mean ± SEM. $P < 0.05$ and $P < 0.01$.

CDCA enhances anti-inflammatory cascades mediated via M2-type macrophage polarization

The data from M2 macrophage marker assays are shown in **Figure 9**. Compared with the untreated healthy group, the levels of mRNA encoding CD206 and CD163 were strikingly lower in the FLHS model group ($P < 0.01$). In contrast, the mRNA expression level of ARG showed no statistically significant shift. After animals received CDCA, transcript abundance for CD206, CD163, and ARG increased substantially above that in the control group ($P < 0.01$).

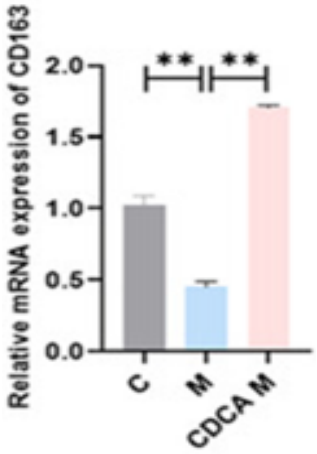

a)

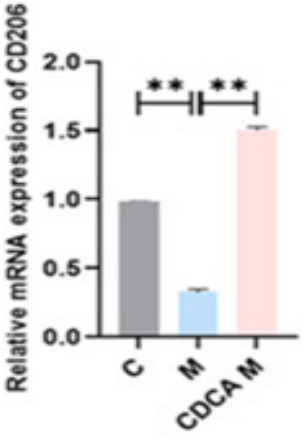

b)

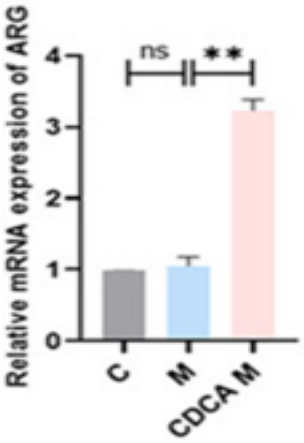

c)

Figure 9. Profiling of macrophage identity markers in hepatic tissue from laying hens: (a) Changes brought about by CDCA in CD163 gene transcript abundance within FLHS hens, (b) Changes in CDCA-induced CD206 gene transcript abundance in FLHS hens, and (c) Changes in CDCA-induced ARG gene transcript abundance in FLHS hens. Data plotted as mean ± SEM. $P < 0.01$, and ns ($P > 0.05$).

The determinations of M2-polarized macrophage-linked effector molecules are depicted in **Figure 10**. The FLHS model cohort showed a pronounced depletion of both IL-4 and IL-10 compared with the normal untreated cohort ($P < 0.01$). In the wake of the CDCA provision, however, these two cytokines rebounded sharply, reaching significantly higher levels than those observed in the control cohort ($P < 0.01$).

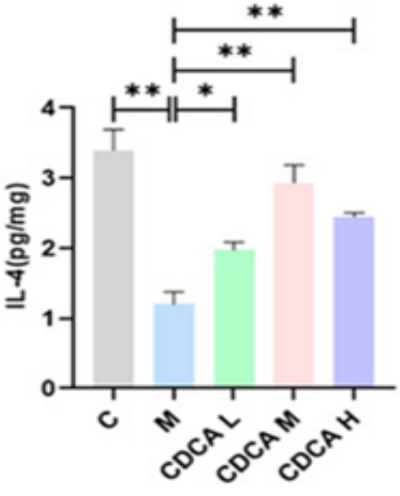

a)

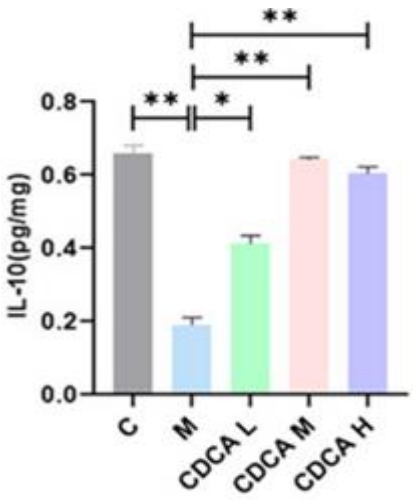

b)

Figure 10. Quantification of inflammation-resolving mediators within the livers of laying hens: (a) Influence of CDCA on intrahepatic IL-4 concentrations in FLHS laying hens, and (b) Influence of CDCA on intrahepatic IL-10 concentrations in FLHS laying hens. All values represent mean ± SEM. $P < 0.05$ and $P < 0.01$.

Figure 11 displays the outcomes of examining multiple regulatory components within signaling cascades governed by M2-polarized macrophages. Compared with the normal control cohort, transcript abundance of IL-4R and SOCS1 was notably diminished in the FLHS model cohort ($P < 0.05$). Conversely, mRNA expression of PPAR-γ and KLF4 was markedly elevated relative to the control cohort ($P < 0.05$), whereas STAT6 transcript levels did not differ significantly. After CDCA intervention, the mRNA levels of IL-4R, PPAR-γ, KLF4, STAT6, and SOCS1 increased significantly ($P < 0.01$).

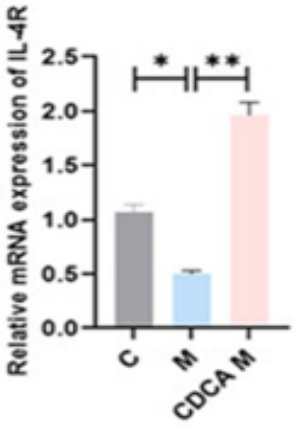

a)

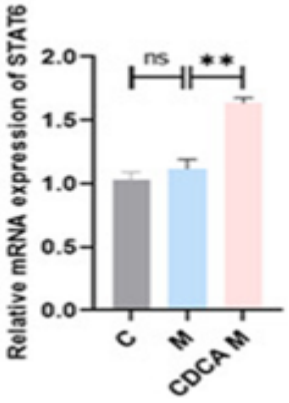

b)

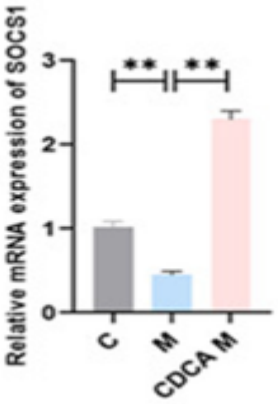

c)

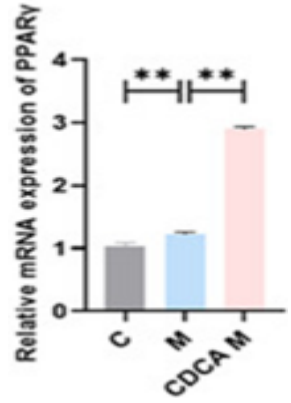

d)

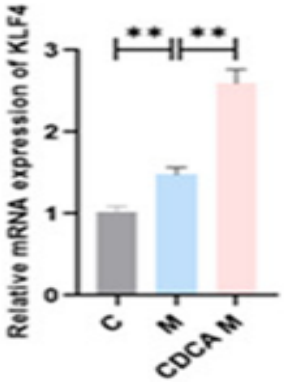

e)

Figure 11. Profiling of regulatory nodes within the signal transduction route linked to M2-type macrophages: (a) Alterations in hepatic IL-4R gene transcript levels elicited by CDCA in FLHS hens, (b)

Alterations in hepatic STAT6 gene transcript levels elicited by CDCA in FLHS hens, (c) Alterations in hepatic SOCS1 gene transcript levels elicited by CDCA in FLHS hens, (d) Alterations in hepatic PPARγ gene transcript levels elicited by CDCA in FLHS hens, and (e) Alterations in hepatic KLF4 gene transcript levels elicited by CDCA in FLHS hens. Data plotted as mean ± SEM. $P < 0.05$, $P < 0.01$, and ns ($P > 0.05$).

FLHS constitutes a widespread metabolic-nutritional ailment of laying hens and tends to arise when birds are at the height of their laying cycle. The disorder is characterized by massive lipid deposition and diffuse bleeding within the hepatic parenchyma [9, 10]. Such pathology commonly triggers a precipitous fall in egg yield and a truncated peak production phase, with case fatality proportions in affected flocks ranging from 40 to 70% [11]. A body of work has linked FLHS onset to variables including dietary composition, heritable susceptibility, ambient conditions, husbandry practices, and the gut microbiome [12]. Mechanistically, FLHS mirrors human NAFLD in many respects, yet the finer mechanistic details remain unresolved, and robust preventive or curative measures remain elusive.

Constructing a faithful FLHS model in laying hens is a prerequisite for dissecting disease mechanisms and evaluating prospective countermeasures. Several approaches have been described for inducing FLHS in layers, including exogenous estradiol benzoate administration [13] and manipulation of feed formula ratios [14, 15]. Nevertheless, supplying an energy-dense, protein-restricted ration remains the predominant strategy for producing FLHS model hens, given its relative ease and operational simplicity. The etiopathogenesis, temporal progression, and symptomatic picture in diet-induced FLHS model birds closely parallel those observed in spontaneous FLHS arising in real-world production scenarios.

For this investigation, we built an FLHS model by providing a high-energy, low-protein diet. We noted gross hepatomegaly in FLHS model hens, accompanied by overt hemorrhagic foci. The hepatic tissue was also friable and prone to crumbling upon handling. Microscopic examination of liver sections from FLHS birds disclosed hepatocellular disintegration, loss of distinct hepatic cord architecture, and an accumulation of sizable fatty vacuoles with unmistakable steatotic changes. Circulating ALT and AST enzyme activities rose sharply in FLHS hens, confirming the successful generation of the model. The pathological attributes of our FLHS model hens aligned well with earlier published descriptions [16, 17].

Remedial administration of CDCA led to an overall restoration of hepatic mass and coloration toward normal values in FLHS birds, while bleeding severity was markedly lessened. At the tissue architecture level, the liver of FLHS hens progressively regained a normal appearance after CDCA provision, and the abundance of fatty vacuoles receded. Enzymatic markers ALT and AST in the circulation of FLHS hens fell off significantly post-intervention, suggesting that CDCA substantially attenuates the hepatic insult associated with FLHS in layers. Although specific reports on CDCA easing FLHS in laying hens are absent from the scientific record, both preclinical animal studies and clinical evaluations have established that exogenously delivered bile acids—or their semisynthetic derivatives—can reverse hepatotoxic damage from a variety of origins [18-20]. Fu and collaborators reported that dietary supplementation with obeticholic acid blunted liver injury in NASH mice by reducing cell death [21]. Huang and colleagues demonstrated that CDCA dosing mitigated diet-induced hepatic injury in rats fed a high-fat diet [22]. An investigation by Aljarboa and co-workers determined that CDCA supplementation reduced valproic acid–provoked hepatic toxicity in rats [23].

A multitude of recent investigations have established that during fatty liver disease states, resident hepatic macrophages undergo increased skewing toward the M1 functional phenotype and elaborate a broad spectrum of pro-inflammatory mediators. The subsequent inflammatory cascade unleashed by these molecular agents represents a principal driver of hepatocellular injury in fatty liver conditions [24]. Canonical M1 macrophage identifiers include the scavenger receptor CD68 alongside iNOS, and their robust upregulation potentiates downstream inflammatory and immunologic processes [25]. Macrophages may be committed to M1 polarization upon encountering stimulatory cues such as IFN-γ or LPS, whereupon M1-differentiated macrophages discharge elevated amounts of pro-inflammatory cytokines, including IL-1β, TNF-α, IL-18, IL-6, and IL-8. Supraphysiological production of these mediators within the hepatic milieu can directly activate inflammatory pathways, leading to tissue damage. Moreover, the synthesis of these factors spurs the liberation of iNOS from M1 macrophages, thereby compounding inflammatory hepatocellular injury [26]. Our data revealed that transcript abundance for the hepatic M1 macrophage indicators CD68 and iNOS was appreciably upregulated in FLHS hens, as were protein concentrations of the pro-inflammatory mediators IL-1β, IL-6, IL-8, IL-18, iNOS, and TNF-α, collectively implying that hepatic pathology in FLHS hens is intimately tied to the pro-inflammatory cascade elicited by M1-directed polarization of liver-resident macrophages.

By contrast, both transcript and protein readouts for these pro-inflammatory indices were sharply reduced following CDCA intervention. Levels of IL-18, iNOS, and TNF-α were reduced to levels comparable to those of the control

cohort, suggesting that CDCA mitigates hepatic damage in FLHS layers by repressing the pro-inflammatory program initiated by M1-polarized hepatic macrophages. Mohamed *et al*. [27] reported that CDCA blunts inflammation in high-fat diet–challenged model rats by inhibiting the secretion of pro-inflammatory mediators, including TNF-α and IL-6. Working with maternal and placental tissue isolates from cases of intrahepatic cholestasis of pregnancy, Brenøe and colleagues observed that bile acid exposure restrained M1 macrophage commitment by suppressing the expression of M1-associated markers [28]. Zhuang and collaborators documented that targeted deletion of the bile acid receptor gene Gpbar-1 profoundly accelerated the tempo of macrophage M1 polarization and aggravated acute hepatic damage, inflammatory infiltration, and hepatocyte apoptosis in mice subjected to acute cholestatic liver injury [29].

Recent findings have identified JAK-STAT, LPS-TLR4-MyD88-NF-kB, and NLRP3 as integral participants in macrophage polarization and the attendant outpouring of pro-inflammatory mediators. Upon binding of INF-γ to its cognate receptors (INFR) on the macrophage plasmalemma, activated JAK2 protein is recruited, leading to induction of the transcription factor STAT1, which subsequently switches on the expression of M1 polarization–linked gene programs that promote the release of pro-inflammatory factors, thereby magnifying the inflammatory response and accentuating end-organ and tissue injury [30]. Our assays showed that the abundance of IFN-γ, JAK2, STAT1, and IRF5—regulatory molecules in the JAK2-STAT1 signaling module—was significantly elevated in FLHS hens. Following CDCA treatment, expression of IFN-γ, JAK2, STAT1, and IRF5 was pronouncedly downregulated, suggesting that CDCA suppresses the M1 macrophage–driven pro-inflammatory reaction in the livers of FLHS hens through a mechanism that dampens the JAK2-STAT1 signaling pathway. Zangerolamo and co-workers reported that TUDCA supplementation attenuated inflammatory pathology in the hypothalamus of Alzheimer's disease model mice by inhibiting the activation of signaling intermediates, such as p-JAK2 and p-STAT3 [31]. Attia and collaborators demonstrated that obeticholic acid slowed both the initiation and progression of NASH in mice by downregulating JAK2 [32]. Work by Renga and colleagues showed that STAT1 dimerization induced by IFN-γ led to transcriptional suppression of the bile acid receptor FXR in macrophages and promoted the production of inflammation-linked cytokines [33]. In a murine model of autoimmune hepatitis, Meng and co-authors reported that blockade of JAK2-STAT1 pathway activation substantially abrogated IFN-γ–triggered hepatic inflammatory damage, secondary to hepatocyte apoptosis [34].

The inflammatory reaction, driven by the LPS-TLR4-MyD88-NF-κB signaling axis, also plays a key role in the pathogenic landscape of NAFLD. As a member of the Toll-like receptor gene family, TLR4 becomes engaged upon recognition of LPS and subsequently drives an inflammatory program. Ordinarily, this molecular sequence aids in purging exogenous bacterial toxins [35]; however, when inflammatory activity exceeds homeostatic limits, it can provoke tissue destruction exceeding that caused by the original infectious agent [36]. TLR4 is abundantly expressed across macrophages, monocytes, and dendritic cells and selectively interacts with LPS, triggering signal propagation through downstream effector pathways, prominently including the MyD88-dependent pathway [37, 38]. The MyD88-governed route stands as the chief downstream cascade mobilized by TLR4; it initially recruits IL-1 receptor–associated kinase, after which TRAF6 is engaged to catalyze the phosphorylation of IκB, a step that ultimately permits the nuclear import of a battery of transcriptional regulators such as NF-κB, AP-1, and IRF1 [39]. Once positioned within the hepatic microenvironment, NF-κB launches a succession of signaling events inside M1-skewed macrophages via both MyD88-obligate and MyD88-bypass mechanisms, thereby eliciting the secretion of a multitude of pro-inflammatory mediators that ignite hepatic inflammation.

Within the scope of this investigation, LPS titers were found to be strikingly elevated in FLHS layers, whilst the transcript abundance of TLR4, MyD88, NF-κB, AP-1, and IRF1 was similarly upregulated. In direct opposition to this pattern, the molecular readouts of participants in the LPS-TLR4-MyD88-NF-κB cascade plummeted following CDCA provision, indicating that the manner in which CDCA tempers the M1 macrophage–driven pro-inflammatory response in the hepatic compartment of FLHS hens is mechanistically coupled to the curtailment of LPS-TLR4-MyD88-NF-κB pathway transduction. Working with a rodent model of LPS-provoked hepatic insult, Milivojac and collaborators established that CDCA dosing markedly lessened LPS-instigated liver pathology by driving down circulating LPS levels [40]. Dai and coinvestigators noted that exposing cholangiocarcinoma cells to CDCA suppresses tumor-associated inflammation by repressing the LPS-TLR4-MyD88-NF-κB signaling pathway [41]. Research undertaken by Yang and associates demonstrated that pharmacological stimulation of bile acid receptors reduced hepatic inflammatory tissue damage in ANIT-exposed cholestatic hepatitis mice by lowering LPS bioavailability and interfering with the LPS-TLR4-MyD88-NF-κB signaling module [42]. Mobraten and other researchers have documented that incubation

with bile acids, such as CDCA, impairs NF-κB pathway activation in both U937 cells and freshly isolated human CD14+ monocytes, thereby dampening the cellular inflammatory cascade triggered by LPS [43].

Over the past several years, an expanding body of scientific work has delineated the role of NLRP3 inflammasome–orchestrated inflammatory events in the hepatocellular damage that accompanies metabolism-associated fatty liver disease. Operating as a critical surveillance component of the innate defensive network, NLRP3 senses incursions by foreign microbial products along with endogenous danger signals arising from cellular stress, and its response involves the nucleation of NLRP3 inflammasome multimolecular platforms. During the incipient phase of metabolism-associated fatty liver disease, LPS synthesis escalates dramatically, Kupffer cells and recruited macrophages undergo M1-favored differentiation, and NLRP3 inflammasome complexes gain functional competence, which, in turn, accelerates both transcriptional activation and de novo protein synthesis of inflammasome-associated subunits, namely ASC, Caspase-1, and Caspase-11. This molecular program subsequently facilitates the proteolytic maturation and exocytic discharge of the pro-inflammatory cytokines IL-1β and IL-18, thereby kindling an inflammatory cascade that culminates in inflammation-attributable tissue pathology [44]. The current body of work revealed that mRNA expression levels of NLRP3, Caspase-1, and Caspase-11 were significantly higher in the FLHS group than in the corresponding control group. The abundance of each of these molecular species decreased significantly upon CDCA exposure, indicating that CDCA exerts a direct repressive effect on NLRP3 biogenesis, thereby muting the inflammatory response and alleviating the consequences of inflammation-linked hepatic compromise. In a whole-animal study, Gong and colleagues reported that pharmacological blockade of NLRP3 inflammasome activity via Caspase-1 antagonism reduced IL-1β levels in mouse hepatic tissue, thereby mitigating liver damage associated with fibrotic transformation [45]. In parallel, Oleszycka *et al*. reported that CDCA attenuates LPS-induced inflammatory injury in murine dendritic cells by transcriptionally downregulating NLRP3 and Caspase-1. Experimental evidence from Haoran and co-workers established that systemic delivery of CDCA to mice blunts the functional output of NLRP3 inflammasome complexes and Caspase-1 enzymatic activity, thereby halting the release of pro-inflammatory mediators IL-1β, IL-6, and TNF-α and diminishing tissue damage triggered by stress-related insults [46].

A separate cluster of contemporary NAFLD modeling efforts has shown that the functional engagement of M2-polarized macrophages in NAFLD settings leads to transcriptional repression of cytokine genes and other inflammation-associated loci, thereby constraining the extent of hepatic tissue destruction [47, 48]. The differentiation program that guides macrophages into the M2 state is accompanied by substantial transcriptional induction of the signature molecules CD163, CD206, and ARG, a molecular shift that drives the synthesis and secretion of the inflammation-resolving cytokines IL-10, IL-4, IL-13, and TGF-β, thereby enabling their tissue-protective actions. In this set of experiments, mRNA quantities corresponding to CD163, CD206, and ARG, as well as the protein abundance of IL-4 and IL-10, were found to be sharply curtailed in FLHS hens. This finding intimates a connection between hepatic injury in FLHS layers and the anti-inflammatory machinery mobilized through M2-directed repolarization of the hepatic macrophage pool. Strikingly, CDCA therapy led to substantial elevations in CD163, CD206, and ARG transcript levels, accompanied by marked increases in IL-4 and IL-10 protein concentrations. This outcome indicates that CDCA relieves hepatic pathology in FLHS hens by amplifying the inflammation-counteracting response driven by M2-committed liver macrophages. Grander and coinvestigators determined that Nor UDCA supplementation diminished the ethanol-induced intrahepatic expression of the pro-inflammatory mediators IL-1β and IL-6 while simultaneously attenuating liver damage, an effect mechanistically traced to the facilitated redirection of hepatic macrophage polarization toward the M2 fate [49]. Du and collaborators noted that CDCA exposure promoted macrophage differentiation toward the M2 phenotype by upregulating IL-10 production, a shift that reduced high-fat diet–induced inflammatory pathology across the hepatointestinal tissues of Caenorhabditis elegans [50]. Shao *et al*. [51] described a scenario in which LCA treatment restricts glycolytic catabolism while enhancing mitochondrial oxidative phosphorylation and M2 macrophage commitment, thereby reducing liver injury in a murine hepatic fibrosis model. Liu *et al*. [52] found that CDCA administration steers macrophage differentiation toward the M2 state and mitigates inflammatory tissue damage across multiple organs, including the liver, in mice harboring acute myeloid leukemia.

Complementary lines of investigation have illuminated that M2 macrophage commitment can be launched when IL-4 physically associates with IL-4Rα displayed on the outer face of the cell, an interaction that results in the catalytic activation and tyrosine phosphorylation of STAT6 through the upstream intervention of JAK1 and JAK3 [53], after which activated STAT6 forms functional partnerships with the transcriptional regulators KLF4 and PPAR-γ [54]. An alternate route to M2 macrophage specification can be initiated by STAT3 activation upon

IL-10 ligating the IL-10R complex [55]. Members of the SOCS family, which function as inducible inhibitors of signal propagation, are believed to participate in fine-tuning macrophage polarization by furnishing negative feedback restraint over JAK-STAT signaling intensity [56]. Our experimental data documented a substantial reduction in the mRNA expression of IL-4R, STAT6, SOCS1, PPAR-γ, and KLF4 in FLHS hens. Set against this background, CDCA administration led to a pronounced rebound in the transcript abundance of IL-4R, STAT6, SOCS1, PPAR-γ, and KLF4, supporting a model in which CDCA fosters M2-directed macrophage repolarization and boosts intrahepatic levels of inflammation-resolving mediators in FLHS hens by transcriptionally upregulating factors that populate the JAK-STAT signaling circuit. Chen and associates provided evidence that CDCA palliates hepatic inflammation induced by a high-fat diet in mice by augmenting PPAR-γ–dependent transcriptional activity and concurrently promoting M2 macrophage skewing [57]. Experimental manipulations conducted by Lv and co-workers revealed that THDCA supplementation alleviates pharmacologically modeled inflammatory gut pathology in mice by stimulating increased elaboration of both IL-4 and IL-10 [58]. Published findings from Chen and colleagues established that UDCA treatment exerts negative regulatory control over SOCS1 expression, curtails the extent of STAT phosphorylation, accelerates macrophage reorientation toward the M2 phenotype, and ultimately ameliorates hepatocellular injury in NAFLD mice [59].

Conclusion

The findings derived from this investigation demonstrate that preventive supplementation with CDCA substantially attenuates hepatic injury in FLHS laying hens. This protective outcome is achieved through suppression of M1-type macrophage polarization and the ensuing pro-inflammatory cascade, mediated by downregulation of the JAK-STAT, LPS-TLR4-MyD88-NF-κB, and NLRP3 signaling axes, alongside upregulation of the JAK-STAT pathway to foster M2-type macrophage polarization and the associated anti-inflammatory response. These observations furnish novel mechanistic insights that may help clarify the pathogenic underpinnings of FLHS in laying hens and support the application of CDCA as a prophylactic strategy against FLHS.

Acknowledgments: None

Conflict of interest: None

Financial support: The authors declare that financial support was received for the research, authorship, and/or publication of this article. This work was supported by the National Natural Science Foundation of China (32272965, 32202753, 31972639), the Science and Technology Department of Liaoning Province (2022-BS-170, 2023-MSLH-281).

Ethics statement: The animal study protocol was approved by the Animal Care and Use Committee of Shenyang Agricultural University (protocol code 2019030101).

References

1. Wolford JH, Polin D. Study on fatty liver-hemorrhagic syndrome (FLHS). Poult Sci. 1972;51(5):1707-13.
2. Day CP, James OF. Steatohepatitis: a tale of two "hits". Gastroenterology. 1998;114(4):842-5.
3. Mao N, Yu Y, Lu X, Yang Y, Liu Z, Wang D. Preventive effects of matrine on LPS-induced inflammation in RAW 264.7 cells and intestinal damage in mice through the TLR4/NF-κB/MAPK pathway. Int Immunopharmacol. 2024;143(Pt 2):113432.
4. Li M, Tan J, Zhang R, Gong X, Xie J, Liu C, et al. Sunitinib alleviates hepatic ischemia reperfusion injury by inhibiting the JAK2/STAT pathway and promoting the M2 polarization of macrophages. Immunopharmacol Immunotoxicol. 2024;46(5):672-84.
5. Comeglio P, Morelli A, Adorini L, Maggi M, Vignozzi L. Beneficial effects of bile acid receptor agonists in pulmonary disease models. Expert Opin Investig Drugs. 2017;26(10):1215-28.
6. Oleszycka E, O'Brien EC, Freeley M, Lavelle EC, Long A. Bile acids induce IL-1α and drive NLRP3 inflammasome-independent production of IL-1β in murine dendritic cells. Front Immunol. 2023;14:1285357.
7. Keitel V, Häussinger D. Role of TGR5 (GPBAR1) in liver disease. Semin Liver Dis. 2018;38(4):333-9.
8. Ji CG, Xie XL, Yin J, Qi W, Chen L, Bai Y, et al. Bile acid receptor TGR5 overexpression is associated with decreased intestinal mucosal injury and epithelial cell proliferation in obstructive jaundice. Transl Res. 2017;182:88-102.
9. Miao YF, Gao XN, Xu DN, Li MC, Gao ZS, Tang ZH, et al. Protective effect of the new prepared Atractylodes macrocephala Koidz polysaccharide on fatty liver hemorrhagic syndrome in laying hens. Poult Sci. 2021;100(2):938-48.
10. Wei F, Yang X, Zhang M, Xu C, Hu Y, Liu D. Akkermansia muciniphila enhances egg quality and the lipid profile of egg yolk by improving lipid metabolism. Front Microbiol. 2022;13:927245.

11. Shini A, Shini S, Bryden WL. Fatty liver hemorrhagic syndrome occurrence in laying hens: impact of production system. Avian Pathol. 2019;48(1):25-34.
12. Meng J, Ma N, Liu H, Liu J, Liu J, Wang J, et al. Untargeted and targeted metabolomics profiling reveals the underlying pathogenesis and abnormal arachidonic acid metabolism in laying hens with fatty liver hemorrhagic syndrome. Poult Sci. 2021;100(11):101320.
13. Wang A, Zhang K, Fu C, Zhou C, Yan Z, Liu X. Alleviation effect of conjugated linoleic acid on estradiol benzoate induced fatty liver hemorrhage syndrome in Hy-line male chickens. J Anim Sci. 2023;101:skad045.
14. Yadav KK, Boley PA, Khatiwada S, Lee CM, Bhandari M, Kenney SP. Development of fatty liver disease model using high cholesterol and low choline diet in white leghorn chickens. Vet Res Commun. 2024;48(6):2489-97.
15. Guo H, Zhang X, You M, Shen Y, Zhang S, Li J, et al. Quantitative lipidomics reveals the changes of lipids and antioxidant capacity in egg yolk from laying hens with fatty liver hemorrhagic syndrome. Poult Sci. 2024;103(4):103785.
16. Yang X, Li D, Zhang M, Feng Y, Jin X, Liu D, et al. Ginkgo biloba extract alleviates fatty liver hemorrhagic syndrome in laying hens via reshaping gut microbiota. J Anim Sci Biotechnol. 2023;14:97.
17. Cui Z, Jin N, Amevor FK, Shu G, Du X, Kang X, et al. Dietary supplementation of salidroside alleviates liver lipid metabolism disorder and inflammatory response to promote hepatocyte regeneration via PI3K/AKT/Gsk3-β pathway. Poult Sci. 2022;101(9):102034.
18. Banerjee T, Sarkar A, Ali SZ, Bhowmik R, Karmakar S, Halder AK, et al. Bioprotective role of phytocompounds against the pathogenesis of non-alcoholic fatty liver disease to non-alcoholic steatohepatitis: unravelling underlying molecular mechanisms. Planta Med. 2024;90(9):675-707.
19. Lu H, Ban Z, Xiao K, Sun M, Liu Y, Chen F, et al. Hepatic-accumulated obeticholic acid and atorvastatin self-assembled nanocrystals potentiate ameliorative effects in treatment of metabolic-associated fatty liver disease. Adv Sci (Weinh). 2024;11(17):e2308866.
20. Lu Q, Zhu Y, Wang C, Zhang R, Miao Y, Chai Y, et al. Obeticholic acid protects against lithocholic acid-induced exogenous cell apoptosis during cholestatic liver injury. Life Sci. 2024;337:122355.
21. Fu J, Zhang P, Sun Z, Lu G, Cao Q, Chen Y, et al. A combined nanotherapeutic approach targeting farnesoid X receptor, ferroptosis, and fibrosis for non-alcoholic steatohepatitis treatment. Acta Pharm Sin B. 2024;14(5):2228-46.
22. Huang L, Li Y, Tang R, Yang P, Zhuo Y, Jiang X, et al. Bile acids metabolism in the gut-liver axis mediates liver injury during lactation. Life Sci. 2024;338:122380.
23. Aljarboa AS, Alhusaini AM, Sarawi WS, Mohammed R, Ali RA, Hasan IH. The implication of LPS/TLR4 and FXR receptors in hepatoprotective efficacy of indole-3-acetic acid and chenodeoxycholic acid. Life Sci. 2023;334:122182.
24. Hsu CC, Cheng KC, Li Y, Hsu PH, Cheng JT, Niu HS. TGR5 expression is associated with changes in the heart and urinary bladder of rats with metabolic syndrome. Life (Basel). 2021;11(7):695.
25. Zhang B, Yang Y, Yi J, Zhao Z, Ye R. Hyperglycemia modulates M1/M2 macrophage polarization via reactive oxygen species overproduction in ligature-induced periodontitis. J Periodontal Res. 2021;56(5):991-1005.
26. Sun S, Yao Y, Huang C, Xu H, Zhao Y, Wang Y, et al. CD36 regulates LPS-induced acute lung injury by promoting macrophages M1 polarization. Cell Immunol. 2022;372:104475.
27. Shihabudeen MS, Roy D, James J, Thirumurugan K. Chenodeoxycholic acid, an endogenous FXR ligand alters adipokines and reverses insulin resistance. Mol Cell Endocrinol. 2015;414:19-28.
28. Brenøe JE, van Hoorn EGM, Beck L, Bulthuis M, Bezemer RE, Gordijn SJ, et al. Altered placental macrophage numbers and subsets in pregnancies complicated with intrahepatic cholestasis of pregnancy (ICP) compared to healthy pregnancies. Placenta. 2024;153:22-30.
29. Zhuang L, Jia N, Zhang L, Zhang Q, Antwi SO, Sartorius K, et al. Gpbar-1/cAMP/PKA signaling mitigates macrophage-mediated acute cholestatic liver injury via antagonizing NLRP3-ASC inflammasome. Biochim Biophys Acta Mol Basis Dis. 2024;1870(5):167266.
30. Kayagaki N, Stowe IB, Lee BL, O'Rourke K, Anderson K, Warming S, et al. Caspase-11 cleaves gasdermin D for non-canonical inflammasome signalling. Nature. 2015;526(7575):666-71.
31. Zangerolamo L, Solon C, Soares GM, Engel DF, Velloso LA, Boschero AC, et al. Energy homeostasis deregulation is attenuated by TUDCA treatment in streptozotocin-induced Alzheimer's disease mice model. Sci Rep. 2021;11(1):18114.
32. Attia YM, Tawfiq RA, Gibriel AA, Ali AA, Kassem DH, Hammam OA, et al. Activation of FXR modulates SOCS3/Jak2/STAT3 signaling axis in a NASH-dependent hepatocellular carcinoma animal model. Biochem Pharmacol. 2021;186:114497.

33. Renga B, Migliorati M, Mencarelli A, Fiorucci S. Reciprocal regulation of the bile acid-activated receptor FXR and the interferon-gamma-STAT-1 pathway in macrophages. Biochim Biophys Acta. 2009;1792(6):564-73.
34. Meng C, Liu Y, Ming Y, Lu C, Li Y, Zhang Y, et al. Enhancing liver delivery of gold nanoclusters via human serum albumin encapsulation for autoimmune hepatitis alleviation. Pharmaceutics. 2024;16(1):110.
35. Ciesielska A, Matyjek M, Kwiatkowska K. TLR4 and CD14 trafficking and its influence on LPS-induced pro-inflammatory signaling. Cell Mol Life Sci. 2021;78(3):1233-61.
36. Funes SC, Rios M, Escobar-Vera J, Kalergis AM. Implications of macrophage polarization in autoimmunity. Immunology. 2018;154(2):186-95.
37. Wang L, Yang JW, Lin LT, Huang J, Wang XR, Su XT, et al. Acupuncture attenuates inflammation in microglia of vascular dementia rats by inhibiting miR-93-mediated TLR4/MyD88/NF-κB signaling pathway. Oxid Med Cell Longev. 2020;2020:8253904.
38. Li W, Feng G, Gauthier JM, Lokshina I, Higashikubo R, Evans S, et al. Ferroptotic cell death and TLR4/Trif signaling initiate neutrophil recruitment after heart transplantation. J Clin Invest. 2019;129(6):2293-304.
39. Saikh KU. MyD88 and beyond: a perspective on MyD88-targeted therapeutic approach for modulation of host immunity. Immunol Res. 2021;69(2):117-28.
40. Milivojac T, Grabež M, Krivokuća A, Maličević U, Gajić Bojić M, Đukanović Đ, et al. Ursodeoxycholic and chenodeoxycholic bile acids attenuate systemic and liver inflammation induced by lipopolysaccharide in rats. Mol Cell Biochem. 2024. Online ahead of print.
41. Dai J, Wang H, Dong Y, Zhang Y, Wang J. Bile acids affect the growth of human cholangiocarcinoma via NF-kB pathway. Cancer Invest. 2013;31(2):111-20.
42. Yang T, Li L, Pang J, Heng C, Wei C, Wang X, et al. Modulating intestinal barrier function by sphingosine-1-phosphate receptor 1 specific agonist SEW2871 attenuated ANIT-induced cholestatic hepatitis via the gut-liver axis. Int Immunopharmacol. 2023;125(Pt A):111150.
43. Mobraten K, Haugbro T, Karlstrom E, Kleiveland CR, Lea T. Activation of the bile acid receptor TGR5 enhances LPS-induced inflammatory responses in a human monocytic cell line. J Recept Signal Transduct Res. 2015;35:402-9.
44. Zhao L, Zhang H, Liu X, Xue S, Chen D, Zou J, et al. TGR5 deficiency activates antitumor immunity in non-small cell lung cancer via restraining M2 macrophage polarization. Acta Pharm Sin B. 2022;12(2):787-800.
45. Gong Z, Zhou J, Zhao S, Tian C, Wang P, Xu C, et al. Chenodeoxycholic acid activates NLRP3 inflammasome and contributes to cholestatic liver fibrosis. Oncotarget. 2016;7(51):83951-63.
46. Li H, Zhu X, Xu J, Li L, Kan W, Bao H, et al. The FXR mediated anti-depression effect of CDCA underpinned its therapeutic potentiation for MDD. Int Immunopharmacol. 2023;115:109626.
47. Lai YS Jr, Nguyen HT, Salmanida FP, Chang KT. MERTK+/hi M2c macrophages induced by baicalin alleviate non-alcoholic fatty liver disease. Int J Mol Sci. 2021;22(19):10604.
48. Chen X, Tang J, Shuai W, Meng J, Feng J, Han Z. Macrophage polarization and its role in the pathogenesis of acute lung injury/acute respiratory distress syndrome. Inflamm Res. 2020;69(9):883-95.
49. Grander C, Meyer M, Steinacher D, Claudel T, Hausmann B, Pjevac P, et al. 24-Norursodeoxycholic acid ameliorates experimental alcohol-related liver disease and activates hepatic PPARγ. JHEP Rep. 2023;5(11):100872.
50. Du J, Xiang X, Li Y, Ji R, Xu H, Mai K, et al. Molecular cloning and characterization of farnesoid X receptor from large yellow croaker (Larimichthys crocea) and the effect of dietary CDCA on the expression of inflammatory genes in intestine and spleen. Comp Biochem Physiol B Biochem Mol Biol. 2018;216:10-7.
51. Shao J, Ge T, Tang C, Wang G, Pang L, Chen Z. Synergistic anti-inflammatory effect of gut microbiota and lithocholic acid on liver fibrosis. Inflamm Res. 2022;71(10-11):1389-401.
52. Liu J, Wei Y, Jia W, Can C, Wang R, Yang X, et al. Chenodeoxycholic acid suppresses AML progression through promoting lipid peroxidation via ROS/p38 MAPK/DGAT1 pathway and inhibiting M2 macrophage polarization. Redox Biol. 2022;56:102452.
53. Wu WJ, Wang SH, Wu CC, Su YA, Chiang CY, Lai CH, et al. IL-4 and IL-13 promote proliferation of mammary epithelial cells through STAT6 and IRS-1. Int J Mol Sci. 2021;22(21):12008.
54. Gong T, Yan R, Kang J, Chen R. Chemical components of Ganoderma. Adv Exp Med Biol. 2019;1181:59-106.
55. Nelms K, Keegan AD, Zamorano J, Ryan JJ, Paul WE. The IL-4 receptor: signaling mechanisms and biologic functions. Annu Rev Immunol. 1999;17:701-38.
56. Arnold CE, Whyte CS, Gordon P, Barker RN, Rees AJ, Wilson HM. A critical role for suppressor of

cytokine signalling 3 in promoting M1 macrophage activation and function in vitro and in vivo. Immunology. 2014;141(1):96-110.

57. Chen X, Yan L, Guo Z, Chen Y, Li M, Huang C, et al. Chenodeoxycholic acid attenuates high-fat diet-induced obesity and hyperglycemia via the G protein-coupled bile acid receptor 1 and proliferator-activated receptor γ pathway. Exp Ther Med. 2017;14(6):5305-12.
58. Lv L, Chen Z, Bai W, Hao J, Heng Z, Meng C, et al. Taurohyodeoxycholic acid alleviates trinitrobenzene sulfonic acid induced ulcerative colitis via regulating Th1/Th2 and Th17/Treg cells balance. Life Sci. 2023;318:121501.
59. Chen YS, Liu HM, Lee TY. Ursodeoxycholic acid regulates hepatic energy homeostasis and white adipose tissue macrophages polarization in leptin-deficiency obese mice. Cells. 2019;8(3):253.